

Aerodynamic characteristics of two-dimensional sharp-edged objects in tandem arrangement^{*)}

R. GNATOWSKA

*Institute of Thermal Machinery
Częstochowa University of Technology
42-200 Częstochowa, Poland
e-mail: gnatowska@imc.pcz.czyst.pl*

THE PRESENT ANALYSIS addresses the problem of the aerodynamic loads of two prismatic bodies in tandem arrangement. Two identical square cross-section prismatic bodies arranged in tandem are considered and represent a two-dimensional configuration. The program of the study consists of parallel wind-tunnel experiments and numerical simulation performed with the use of a phase-averaged form of $k-\varepsilon$ turbulence model in RNG version. The simulations revealed a strong dependence between the interference of the wake flow around the system of sharp-edged bluff-bodies, the vorticity structure of the separation region, mean position of the reattachment point, phase-averaged velocity field and skin friction variability. The general aim was to establish a direct link between the flow around bluff bodies, local time-resolved quantities like skin friction and surface pressure, and near-wake behaviour behind the square cylinders in tandem array. In particular, it was found that periodical flow disturbances bring about a rapid growth of surface pressure and wall shear stress fluctuations.

Key words: aerodynamic interference, surface friction, wall shear stress, URANS modelling.

Notations

- AC autocorrelation coefficient, $AC = \overline{x_i(t)x_i(t+\tau)} / \sqrt{\overline{x_i(t)^2}}$,
 B obstacle side dimension, m,
 b_r blockage ratio, %,
 C_D mean drag coefficient, $C_D = D / \frac{1}{2} \rho B \overline{U_\infty^2}$,
 c_f wall shear stress coefficient, $c_f = \tau / \frac{1}{2} \rho \overline{U_\infty^2}$,
 C'_p fluctuating pressure coefficient, $C'_p = p_{RMS} / p_d = \sqrt{\overline{p'^2}} / \frac{1}{2} \rho \overline{U_\infty^2}$,
 D drag, N,
 I_∞ turbulence intensity, %,
 IC intercorrelation coefficient, $IC = \overline{x_i(t)x_j(t+\tau)} / \sqrt{\overline{x_i(t)^2} \overline{x_j(t+\tau)^2}}$,
 Re Reynolds number $B \overline{U_\infty} / \nu$,
 s inter-obstacle distance, m,

^{*)}The paper was presented at XVIII Polish Conference of Fluid Mechanics (KKMP), Jastrzębia Góra, 21–25 September, 2008.

t	time, s,
τ	skin friction, Pa,
T	period of vortex shedding, s,
\overline{U}	mean longitudinal velocity, m/s,
\overline{V}	mean transverse velocity, m/s.

Subscripts and superscripts

∞	parameters of inlet,
1	upstream object,
2	downwind object.

1. Introduction

THE EXPERIMENTAL and numerical simulation of bluff bodies interference have attracted considerable scientific interest during the last decades [3, 4, 11], because of the important implications of the problem in many fields (civil engineering and environmental aerodynamics domains).

The problem of flow about cylinder pairs has attracted a great deal of research experimentally and, more recently, numerically. Results are presented for *tandem* arrangements, in which one cylinder is directly in the wake of the other, *side-by-side* arrangements, in which the cylinders are arranged transversely to the incoming flow, and *staggered* arrangements, in which the cylinders are arbitrarily configured. The flow field, force coefficients, pressure distributions and intensification or suppression of vortex shedding depend highly on the configuration, shape and spacing of the cylinder pair due to both, wake and proximity-induced interference effects. Excellent summaries of results in each of these arrangements can be found in works by ZDRAVKOVICH [19] and SUMNER *et al.* [16, 17]. In order to develop valid modelling for buffeting loading, the flow phenomenology is first investigated via the Strouhal number, induced force coefficients, flow visualisation and spectral analysis.

Many studies have considered the interference phenomenon for two-dimensional (2D) and three-dimensional (3D) bodies. 2D obstacles of sufficient span to neglect the end-effects are traditionally modelled as prisms or cylinders immersed in a uniform oncoming stream. The 3D configuration includes all cases for which end effects are significant [13, 15]. Due to their practical relevance, this study focuses on wall-mounted geometries. These flows differ from 2D cases due to the advection of upstream vorticity in the oncoming boundary layer and the existence of mean streamwise vortices, which strongly influence momentum transfer normal to the main stream. The studies [4-6] suggest that flows for two- and three-dimensional configurations share many qualitative similarities even though the mean flow structure may be dramatically different.

Most of the previous research on 2D geometries has concentrated on circular cylinders [8, 16, 17, 19]. ZDRAVKOVICH [19] provides an extensive review for

two identical circular cylinders in tandem and identifies several flow regimes as a function of inter-obstacle spacing. These flow patterns have been extensively investigated by several authors, including SUMNER *et al.* [16, 17], LIN *et al.* [10], JESTER and KALLINDERIS [7] and ALAM *et al.* [1, 2] and the references therein, dealing with several aspects of the unsteady flow past circular cylinders arrangement. While structures with circular cross-sections suffer mainly from the vortex resonance type of flow-induced instability, structures with fixed flow separation positions, which include square or rectangular cross-sections, suffer from both the vortex resonance and galloping. This makes the problem of the stability of square or rectangular cylinders a very challenging one. A two-dimensional tandem arrangement of two square cylinders represents an idealization of the flow interference that occurs in an array of cylinders. A number of previous studies: HANGAN *et al.* [3], HAVEL *et al.* [4], JARZA *et al.* [5], LUO *et al.* [12] and MORYN *et al.* [14] have shown mainly the mean characteristics of the flow and mean pressure loading, depending on bluff-body arrangement. Unsteady phenomena are relatively less recognized, particularly for the case of more complex configurations. Nevertheless the vorticity structure, oscillating velocity components present in the flow accompanied by periodical events like vortex shedding, vortex resonance and galloping, are the main problems of the flow-induced instability of square or rectangular cylinders – very challenging for the further studies [19].

Numerical investigations on the flows around a pair of cylinders have also been reported (see [7, 8]). Most of these numerical studies investigated the flow characteristics at low Re (less than 10^3). On the contrary, many experimental studies have been undertaken at Re higher than those at which the numerical studies have been tried. Numerous studies employ qualitative or quantitative flow visualization techniques such as laser Doppler velocimetry (LDV) and PIV technique, to analyze the near-wake flow field [9, 18].

The main purpose of the present paper is to study the influence of the wake on the aerodynamic characteristics of sharp-edged bluff-bodies in tandem arrangement in uniform flow. A tandem arrangement of two cylinders represents an idealization of the flow interference, which occurs in an array of objects. The discussion is partially based on the results of the previous data contained in work of JARZA and GNATOWSKA [5], which revealed different flow regimes and critical body spacing at which drag coefficient and vortex shedding alter rapidly, reflecting the stability mode change.

The experimental modeling of the flow around the body tandem arrangement was supported and extended with numerical simulations performed with the use of the phase-averaged form of the $k-\varepsilon$ model in RNG version, which have shown overall changes in flow pictures observed for increasing spacing ratio s/B . The interaction effects on the surface pressure distributions and also on the wall shear

stress in the context of wind erosion have been studied. The main attention has been paid to the recognition of the interference of the wake flow around the system of sharp-edged bluff-bodies with distribution of surface pressure and wall shear stress fluctuations.

2. The methods of analysis

The program of the study consists of wind-tunnel experiments and numerical simulation performed with the use of a phase-averaged form of the $k - \varepsilon$ turbulence model in RNG version.

The experiments were carried out in an open-circuit wind tunnel at the Institute of Thermal Machinery of the Czestochowa University of Technology (Fig. 1). The test section was $0.5 \text{ m} \times 0.5 \text{ m}$ ($W \times H$) and $\approx 4 \text{ m}$ long. All the measurements were carried out for the free stream velocity $\overline{U}_\infty = 8.3 \text{ m/s}$, inflow turbulence intensity $I_\infty = 1.5\%$ and obstacle side dimension $B = 0.04 \text{ m}$. The Reynolds number based on prism cross-section dimension was $\text{Re} = 22000$. End plates were used to eliminate the tunnel boundary layer effect. The inter-obstacle gap s was changed in the range of non-dimensional values $s/B = 2 \dots 10$. The system of bluff bodies was positioned 1.5 m from the entrance to the working section, perpendicular to the free-stream direction. Thus, the geometry of the body-wind tunnel system was determined by the value of tunnel blockage ratio $b_r \approx 8\%$.

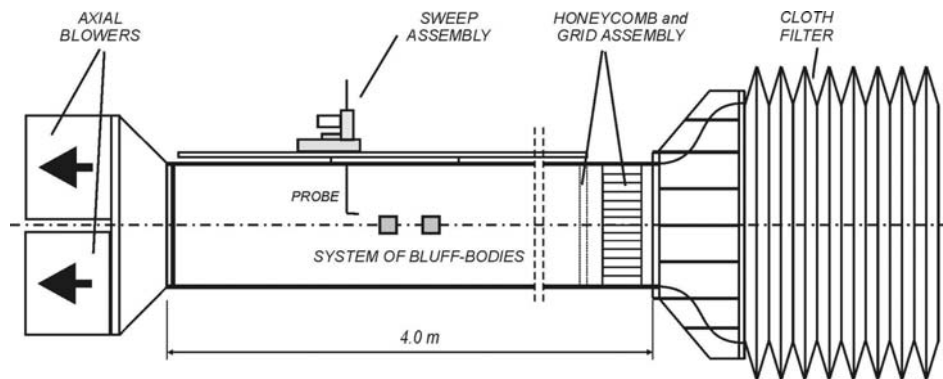


FIG. 1. Two-dimensional channel flow with the system of bluff-bodies.

In the frame of experiments in our wind tunnel, the interaction effects on the surface pressure distributions have been studied. A set of differential pressure transducers was applied to acquire the pressure simultaneously at different locations on the bodies surfaces. To acquire the instantaneous pressure signals on the bodies surfaces, pressure tapings were connected to Honeywell transducers mounted outside the model (type DC001NDR5) having a frequency response of

about 2.0 kHz, which was well above the frequency range of the present investigation. The time traces of pressure signals on the bodies surfaces in the points 1÷11 (see schematic diagram shown in Fig. 2) created the data base for spectral and correlation analysis of pressure fluctuations in flow around tandem arrangement.

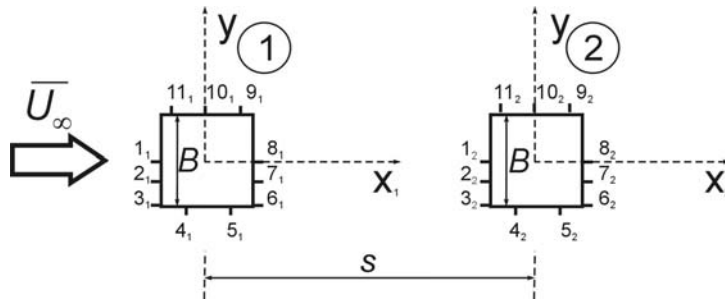


FIG. 2. Two square cylinders in a tandem arrangement. Schematic diagram of surface pressure measuring points locations: (1₁-11₁) for the upwind and (1₂-11₂) for the downwind body.

The experimental modeling of the flow around the bodies in tandem arrangement have been additionally supported and extended by numerical simulations which have shown an overall change in flow pictures observed for increasing spacing ratio s/B . In frame of numerical part of the study, the 2D unsteady RANS simulations were carried out by the use of the $k - \varepsilon$ turbulence model in RNG version. A commercial CFD code FLUENT 6.0 was applied to solve the phase – averaged form of the equations of motion. Pressure-velocity coupling was performed by the SIMPLEC algorithm with the general accuracy of procedure of second order in time and space. The choice of the time step was based on the estimation (through experimental evidence) of the period of flow oscillations. About 50 time steps per period were necessary to obtain the convergence of pressure and velocity – both averaged and RMS values. The time step in dimensionless unit ($t\overline{U_\infty}/B$) was about 0.04 in the present computations. Numerical experiments comprised modelling of unsteady wind conditions in flow approaching the objects in tandem arrangements and surface wall shear stress.

3. Discussion of the results

3.1. Characteristics of instantaneous velocity field

The original contribution of the study presented in previous papers of JARŹA and GNATOWSKA [5, 6] was the recognition of several flow regimes for which the principal differences are due to the interaction between the separated shear layer from the first obstacle and the reattachment and impingement pattern on the faces of downstream body. The obtained results revealed that time characteris-

tics of both, the velocity and pressure field can be grouped in separate classes based on the body spacing, according to the observed flow regimes (single-body, bi-stable, critical, quasi-isolated).

The results of numerical simulation shown in Fig. 3 present the instantaneous isolines of velocity in the flow around bluff bodies. They revealed the changes in

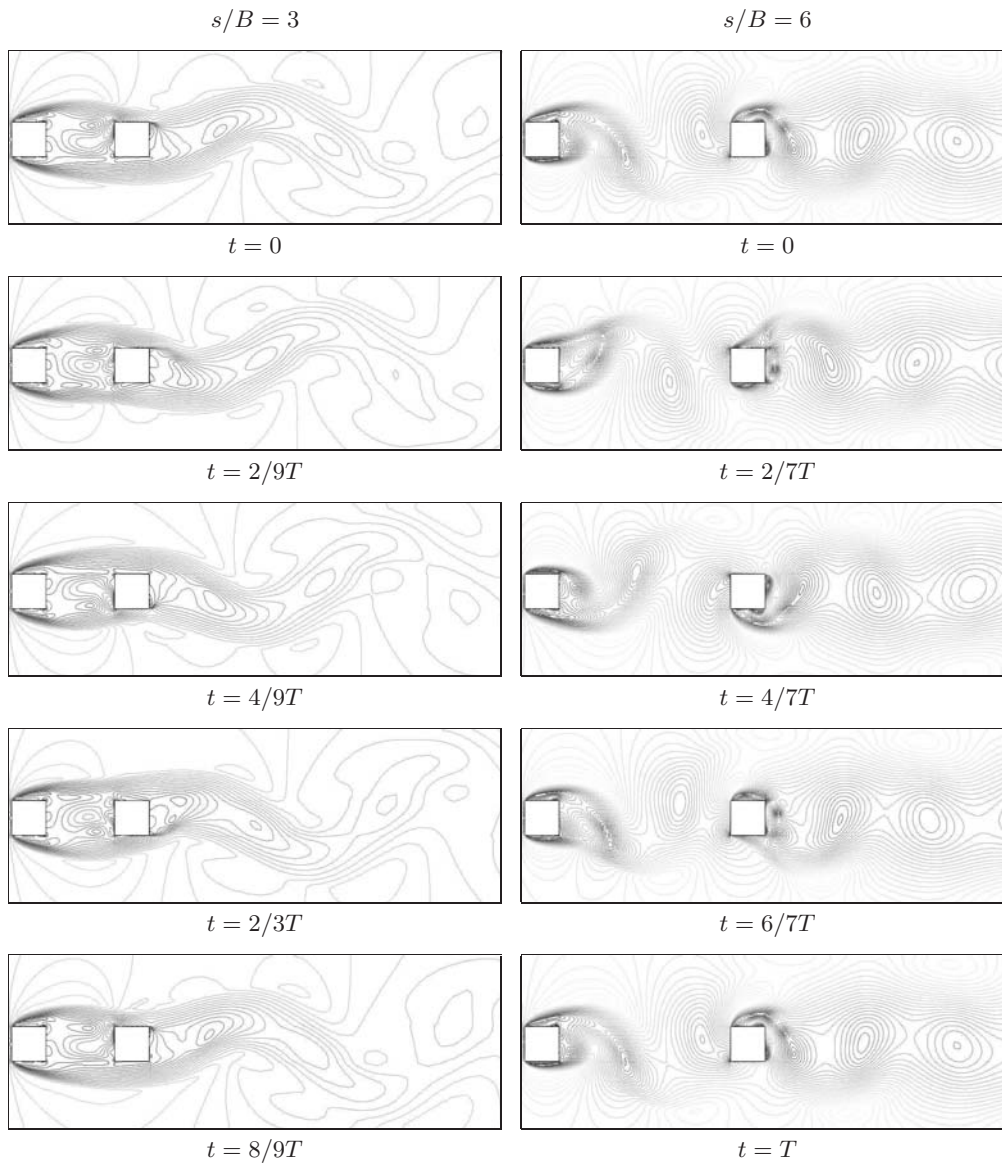


FIG. 3. Unsteady numerical simulation – instantaneous isolines of velocity in one cycle of vortex shedding around obstacles for inter-body spacing $s/B = 3$ and $s/B = 6$.

velocity fields observed as a function of gap width. Two distinct flow patterns are visible here. In the case $s/B = 3$ (Fig. 3) bi-stable regime can be observed with overshooting and reattachment phase, for which the flow intermittently slides off the trailing edge of downwind obstacle and causes alternate vortex shedding. The flow pattern changes gradually as the vortex forming process develops in the inter-body space. For the dimensionless distance $s/B = 6$ (Fig. 3) one can observe the periodical changes of the flow asymmetry in the gap. When the spacing reaches the critical value $s/B \approx 4$, the intermittent switching between flow patterns recognized both for $s/B = 3$ and $s/B = 6$ can be observed. With increasing of s/B , the flow pattern changes gradually as the distance s/B increases, tending to quasi-isolated regime.

3.2. Characteristics of instantaneous pressure loading

The above-mentioned study revealed that the flow pattern around two tandem cylinders, depending strongly on the body distance, changes rapidly from one stable mode to another. As a result, the experimental pressure loading acting on the prisms was found to jump discontinuously for a spacing ratio above the critical value. It can be seen in Fig. 4 taken from [5], which illustrates the variation of the mean drag C_D as well as in Fig. 5 the fluctuating pressure coefficients C'_p for various body spacings.

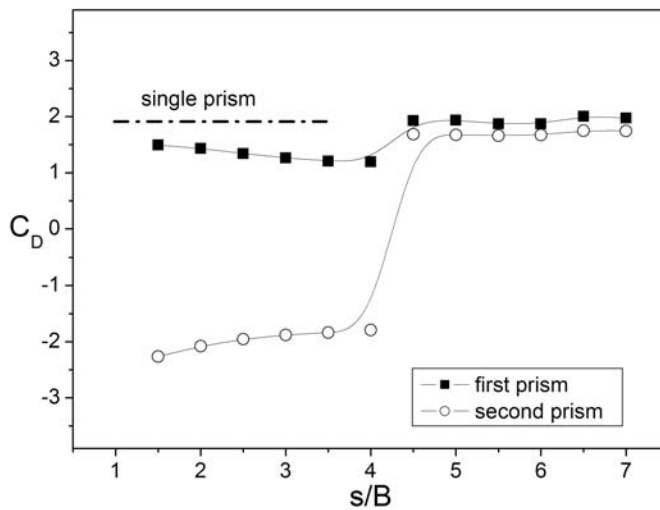


FIG. 4. Distribution of mean drag coefficient for various bodies spacing (s/B) – results of wind-tunnel experiments.

For the upstream prism (Fig. 4), the drag coefficient C_D decreases slowly in function of s/B until it exceeds critical value $s/B \approx 4$. Then C_D starts to

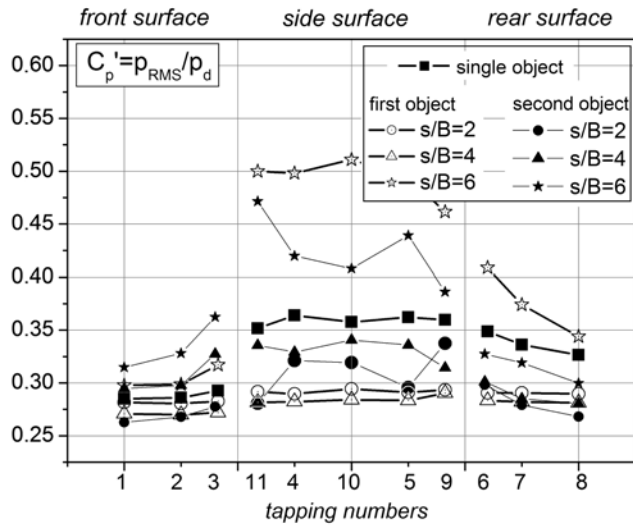


FIG. 5. Surface distributions of fluctuating pressure coefficient on upwind and downstream object for various inter-body spacing – results of wind-tunnel experiments.

increase, tending to the level characteristic for a single body. On the other hand, the downstream body experiences a strong negative drag force, which is sharply reduced for smaller distances s/B . This behavior indicates that the negative pressure on the rear surface is small compared to that on the front surface, influenced by the shear layer separated from the upstream prism. When s/B exceeds the critical value, the drag coefficient increases monotonically, however, even at large body spacing C_D exhibits a smaller value than that obtained for a single prism.

Figure 5 shows the rms values of fluctuating pressure coefficients C'_p measured for various body spacings on the surfaces of the upstream and downstream cylinder in tandem arrangement. The experimental data presented here revealed significant changes in the fluctuating pressure acting on the cylinders for spacing ratios above and below the critical value $s/B \approx 4$. At critical spacing ($s/B \approx 4$) the fluctuating pressure acting on both prisms was found to increase rapidly to reach its maximum value for $s/B = 6$. For the upstream cylinder, the higher level of pressure fluctuations observed on the side and rear faces may be attributed to their proximity to the shear layers separated from the edges. The lower C'_p values are the consequence of weak vortex shedding. The downstream cylinder is subject to impingement of the vortices formed between the two prisms (see Fig. 3). As a result, the value of C'_p starts to rise along the front face and reaches maximum on the side face near the leading edge of the cylinder.

The influence of bluff-bodies arrangement on time traces of pressure signals, expressed in form of a correlation function, is visible in Fig. 6. These results show that characteristics of the pressure surface can be grouped in distinct classes based on the body spacing. The correlation functions provide also evidence for periodical nature of the velocity signal around interfering square cylinders, except for the distances s/B nearly identical to the previously recognized ones as critical spacing. It implies that the mode change is associated with the disturbance of an existing structure of coherent vortices in the flow surrounding the body arrangement (see Fig. 3).

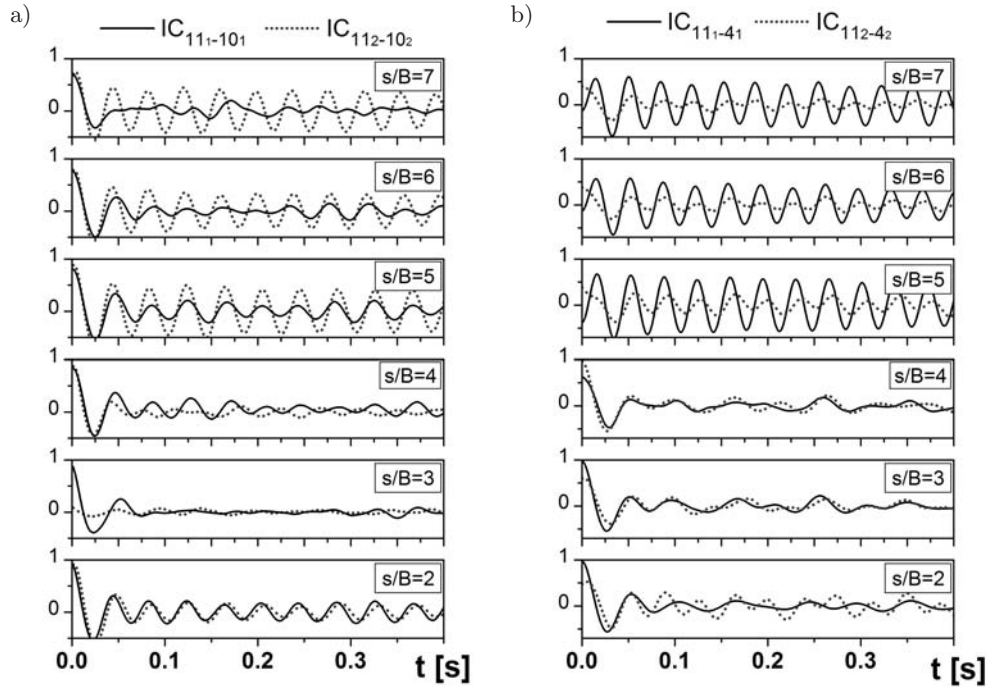


FIG. 6. Intercorrelations (IC) between pressure signals obtained experimentally at positions 11-10 (a) and 11-4 (b), the pressure taps on the walls of two bodies in tandem arrangement.

For the small inter-body spacing the pressure signals periodicity originates here from the wake oscillations transferred through the recirculation zone developed along the side walls of the bodies set of (Fig. 2). That process cannot be related to vortex shedding from the upstream object, because no regular vortex street is formed in the gap. In a bistable regime (distances above the critical spacing) the phase differences are observed, indicating the alternating vortex formation and shedding from the downstream obstacle.

Evidence that vortices are formed and shed from the downstream prism in an alternating fashion is also provided from measurements of the surface pressure fluctuations on the object's faces. The alternate formation of the vortices is confirmed by Fig. 6a, showing the intercorrelation function of the pressure signals from taps 11 and 10, located on the same faces of the upstream and downstream objects (see scheme Fig. 2). Also, the intercorrelation function for the signals from taps 11 and 4 on opposite sides of the bodies (IC11-4) is plotted in Fig. 6b. The data presented here deal with different inter-body spacing. They are related to the upstream as well as to the downstream prism. The intercorrelation function (IC11-10) reveals that the pressure signals over the entire one-side faces of the objects are in phase and nearly identical to AC11, which implies that the motion over the side walls of the tandem arrangement is highly coherent. This conclusion refers to the smaller gap width ($s/B = 4$), as well as to the bigger inter-body distance ($s/B = 6$). The intercorrelation for taps located on the opposite faces (IC1-4) does not reveal any phase difference for the case of tandem arrangement with $s/B = 4$. These observations are consistent with the statement derived from the correlation of HW velocity signals and indicate that for the small inter-body distance, the flow oscillates in phase with the same frequency over the entire space around interfering bodies [5].

On the other hand, an increase of the inter-obstacle gap causes the change of flow regime. As a result, one can observe the phase shift of the intercorrelation function IC11-4 obtained for the pressure signals from the opposite side walls of the tandem arrangement for distances up to $s/B = 5$. It coincides well with the synchronization regime with alternating vortex formation and shedding process from the upstream and downstream prisms (see Fig. 3).

3.3. Characteristics of instantaneous wall shear stress

All the changes of the flow features in the close vicinity of the cylinder surface should be analysed as a complex phenomenon with an important role played by vortex shedding and formation. For the understanding of the shear flows over solid walls in the thin region next to the surface, the knowledge of the wall shear stress is very important. From the distributions of the skin friction the information about the position of the separation points, separation bubbles or transition points can be derived.

The influence of flow patterns around two tandem cylinders on the behavior of the averaged skin friction distributions obtained as a result of the numerical simulation is strongly marked on side face first object (Fig. 7a, c and Fig. 8a, c) and front face second object (Fig. 7b, d and Fig. 8b, d). Diagrams revealed a well-known behavior visible on first and second objects as a function of gap width. The skin friction reaches zero at the stagnation point, peaks near the corners,

drops from them on and achieves its negative values in the separation region. The separation is indicated by vanishing of the skin friction. The results just discussed, combined in diagrams in Figs. 7 and 8, show a sharp decrease towards the value of zero near the corners. The changes in boundary layer evolution around cylinder are especially visible in the regimes with $s/B > 4$. For the close mutual location of interfering objects, the streamlines overshoot (omit) the inter-body space. Therefore, for small distances s/B the gap region is characterized by very low momentum flow. With an increasing s/B , the flow deficit in gap area becomes smaller, due to rolling of shear layers separated from the leading edge of upstream obstacle into the inter-body space. The flow pattern changes gradually as the distance s/B increases, tending to a quasi-isolated regime.

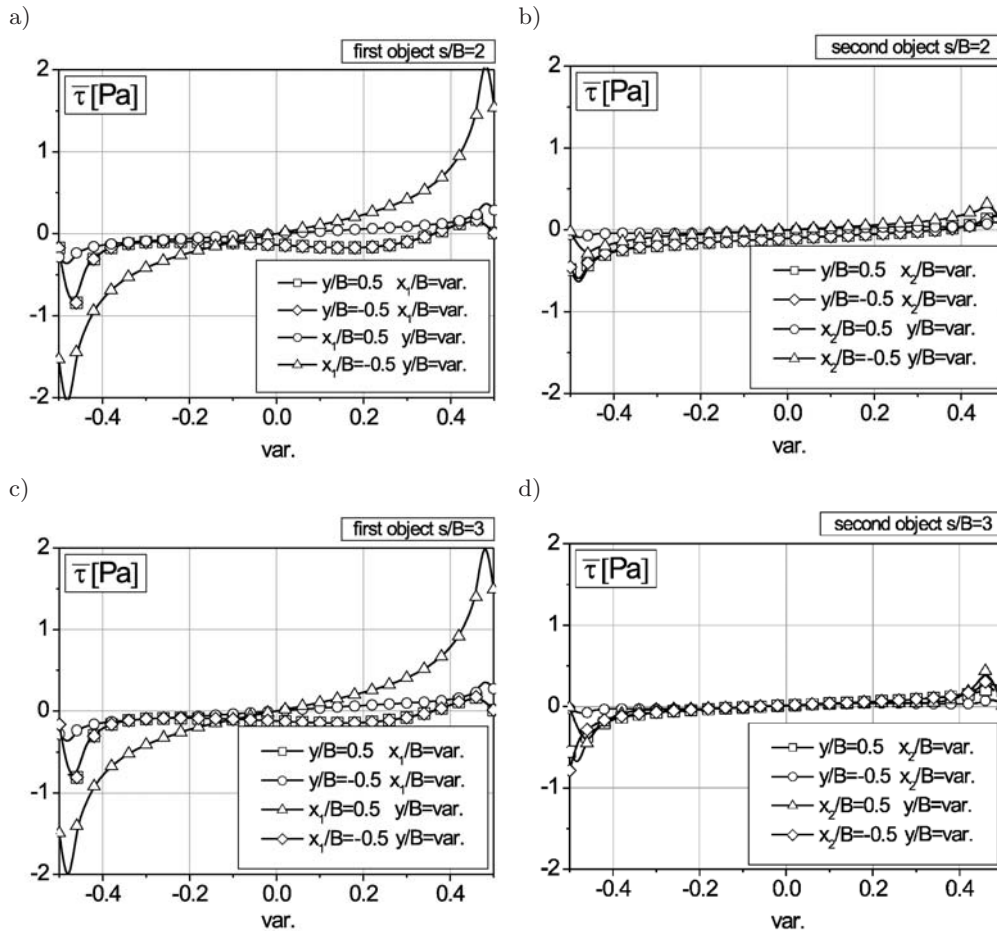


FIG. 7. Distribution of mean skin friction ($\bar{\tau}$) obtained from numerical simulation on walls first (Fig. a and Fig. c) and second (Fig. b and Fig. d) objects for different parameters gap width $s/B = 2$ and $s/B = 3$.

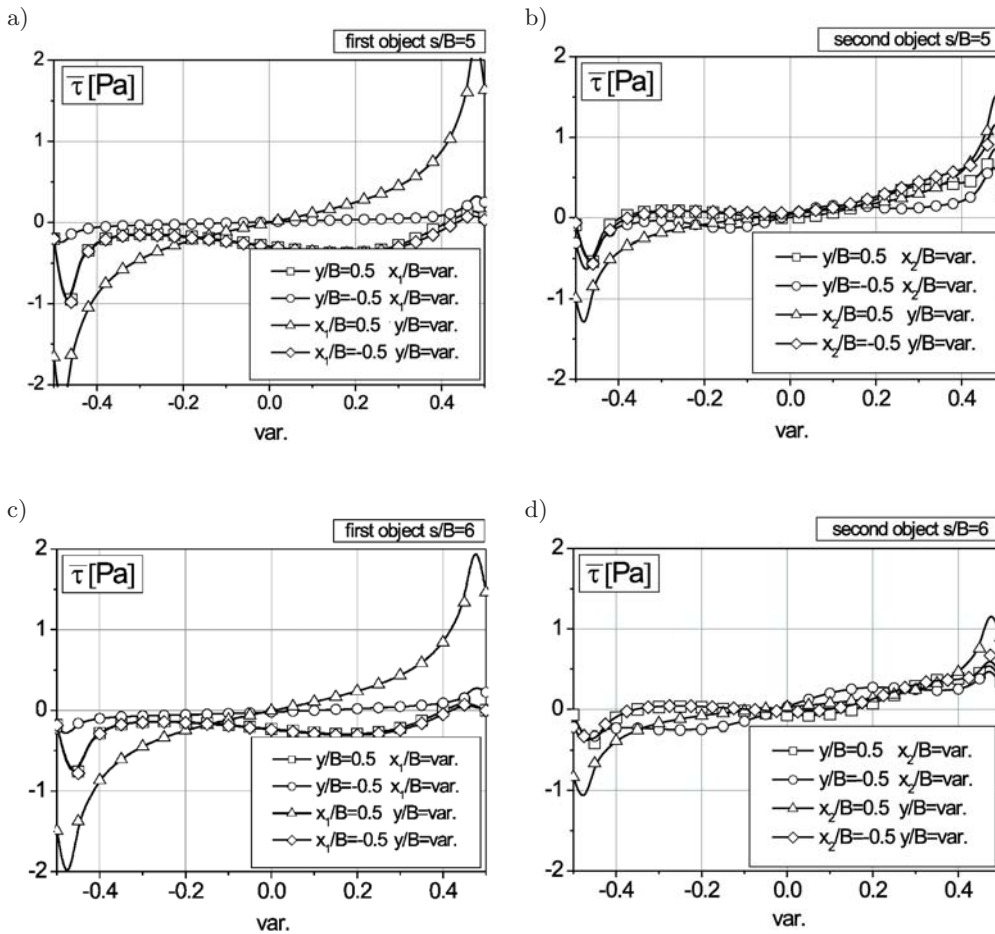


FIG. 8. Distribution of mean skin friction (τ) obtained from numerical simulation on walls first (Fig. a and Fig. c) and second (Fig. b and Fig. d) objects for different parameters gap width $s/B = 5$ and $s/B = 6$.

The sample results of numerical simulation of the instantaneous skin friction distributions over the cylinder surfaces given in the time-space form distributions, made it possible to analyse that problem important also for modelling of the erosion processes. Figures 9 and 10 show the time dependence of instantaneous values of wall shear stress coefficient for front and side faces of the second prism in tandem arrangement.

One may conclude that the location of separation is variable in time and space, undergoing oscillations around the position indicated by the zero value of mean skin friction coefficient.

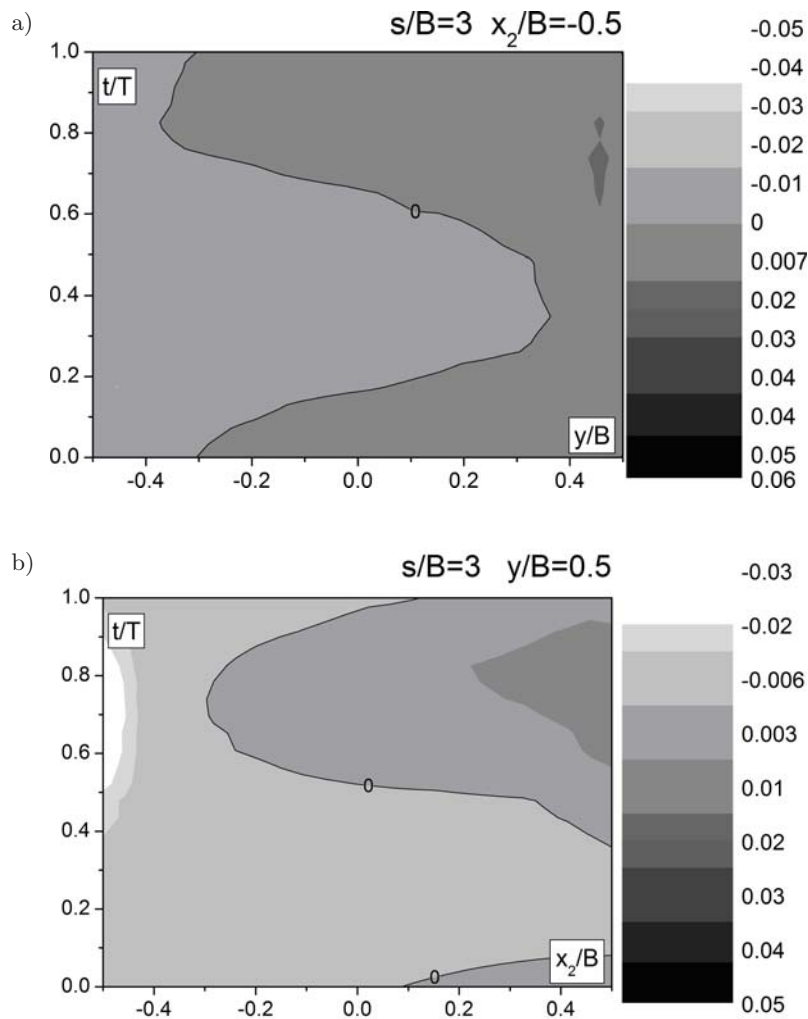


FIG. 9. Time-space distributions of wall shear stress coefficient ($\langle c_f \rangle = \bar{c}_f + \tilde{c}_f(t)$) obtained from numerical simulation for front (a) and side (b) faces of second prism in tandem arrangement $s/B = 3$.

It is interesting to compare the mutual relation between the mean skin friction ($\bar{\tau}$), fluctuating pressure coefficients C'_p and skin friction fluctuations coefficient ($\langle c_f \rangle = \bar{c}_f + \tilde{c}_f(t)$) for the small inter-body spacing and distances above the critical regime. The occurrence of a maximum of C'_p in regimes for $s/B > 4$ is associated with vortex formation and shedding in the gap. Periodic flow disturbances bring about more intensive surface pressure and skin friction oscillations. One can see a rapid growth of pressure and skin friction fluctuations near the separation point (corners) indicated by a zero value of the mean skin friction.

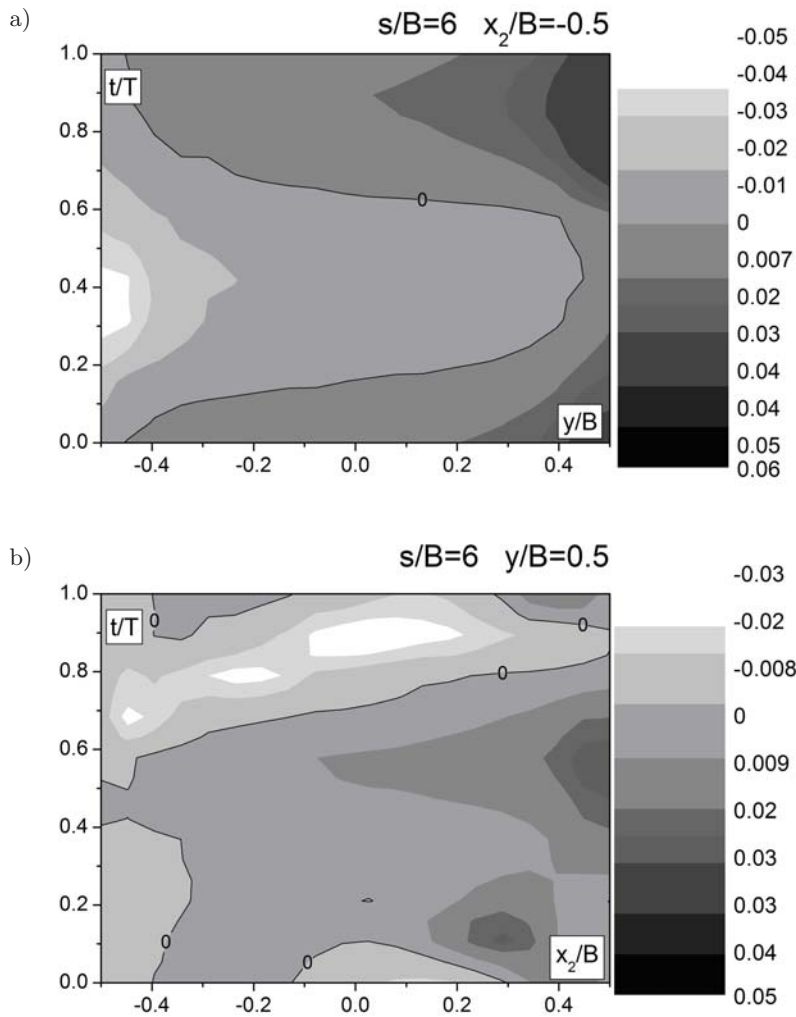


FIG. 10. Time-space distributions of wall shear stress coefficient ($\langle c_f \rangle = \bar{c}_f + \tilde{c}_f(t)$) obtained from numerical simulation for front (a) and side (b) faces of second prism in tandem arrangement $s/B = 6$.

4. Concluding remarks

Two parallel methods were used in the presented research: wind-tunnel experiments and numerical simulation. Experimental measurements served the current verification of numerical calculations before undertaking a more detailed analysis. The combination of two research methods improved efficiency of the conducted investigations.

The general aim was to establish a direct link between the near-wake behaviour around the array of circular cylinders, local time-resolved quantities like skin friction and surface pressure. In particular it was found that the periodical wake flow disturbances bring about more intensive surface pressure and skin friction fluctuations. A rapid growth of pressure and wall shear stress fluctuations has been noticed. Therefore, the changes in boundary layer evolution around cylinders in tandem configuration are especially visible in the synchronisation regime.

Summing up, the present research has confirmed previous suggestions that the vortex forming and turbulence structure in the near-wake-flow can be modified in promising ways through a change of the distance between objects.

References

1. M.M. ALAM, M. MORIYA, K. TAKAI, H. SAKAMOTO, *Fluctuating fluid forces acting on two circular cylinders in a tandem arrangement at a subcritical Reynolds number*, Journal of Wind Engineering Industrial Aerodynamics, **91**, 139–154, 2003.
2. M.M. ALAM, Y. ZHOU, *Phase lag between vortex sheddings from two tandem bluff bodies*, Journal of Fluids and Structures, **23**, 2, 339–347, 2007a.
3. H. HANGAN, B.J. VICKERY, *Buffeting of two-dimensional bluff bodies*, Journal of Wind Engineering and Industrial Aerodynamics, **82**, 173–187, 1999.
4. H. HAVEL, H. HANGAN, R. MARTINUZZI, *Buffeting for 2d and 3d sharp-edged bluff bodies*, Journal of Wind Engineering and Industrial Aerodynamics, **89**, 1369–1381, 2001.
5. A. JARZA, R. GNATOWSKA, *Interference of unsteady phenomena in flow around bluff-bodies arrangement*, Chemical and Process Engineering, **27**, 3/1, 721–735, 2006.
6. A. JARZA, R. GNATOWSKA, *Lock-on effect on unsteady loading of rigid bluff-body in tandem arrangement*, Proceedings of International Conference Urban Wind Engineering and Buildings Aerodynamics COST C14, Rhode-St-Genese Belgium C.2.1-10, 2004.
7. W. JESTER, Y. KALLINDERIS, *Numerical study of incompressible flow about fixed cylinder pairs*, Journal Fluids and Structures, **17**, 557–567, 2003.
8. T. KITAGAWA, H. OHTA, *Numerical investigation on flow around circular cylinders in tandem arrangement at a subcritical Reynolds number*, Journal of Fluids and Structures, **24**, 680–699, 2008.
9. V. KOLAR, D.A. LYN, W. RODI, *Ensemble-average measurements in the turbulent near-wake of the two side-by-side square cylinders*, Journal of Fluid Mechanics, **346**, 201–237, 1997.
10. J.C. LIN, Y. YANG, D. ROCKWELL, *Flow past two cylinders in tandem: instantaneous and averaged flow structure*, Journal of Fluids and Structures, **16**, 1059–1071, 2002.
11. CH.-H. LIU, M.CH. JERRY, *Observations of hysteresis in flow around two square cylinders in a tandem arrangement*, Journal of Wind Engineering and Industrial Aerodynamics, **90**, 1019–1050, 2002.

12. S.C. LUO, T.C. TENG, *Aerodynamic forces on a square section cylinder that is downstream to an identical cylinder*, J. Aeronaut., **94**, 203–212, 1990.
13. R. MARTINUZZI, B. HAVEL, *Turbulent flow around two interfering surface-mounted cubic obstacles in tandem arrangement*, Trans. ASME J. Fluids Eng., **122**, 24–31, 2000.
14. E. MORYN-KUCHARCZYK, R. GNATOWSKA, *Pollutant dispersion in flow around bluff-bodies arrangement*, Wind Energy Springer-Verlag, Berlin, 49–53, 2007.
15. H. SAKAMOTO, H. HANIU, *Effect of free-stream turbulence on characteristics of fluctuating forces acting on two square prisms in tandem arrangement*, J. Fluids Eng., **110**, 140–146, 1988.
16. D. SUMNER, S.J. PRICE, M.P. PAÏDOUSSIS, *Tandem cylinders in impulsively started flow*, Journal of Fluids and Structures, **13**, 955–965, 1999.
17. D. SUMNER, M.D. RICHARDS, O.O. AKOSILE, *Two staggered circular cylinders of equal diameter in cross-flow*, Journal of Fluids and Structures, **20**, 255–276, 2005.
18. S.C. YEN, K.C. SAN, T.H. CHUANG, *Interactions of tandem square cylinders at low Reynolds numbers*, Experimental Thermal and Fluid Science, **32**, 927–938, 2008.
19. M. ZDRAVKOVICH, *Review of flow interference between two circular cylinders in various arrangements*, ASME Journal of Fluids Engineering, **99**, 618–633, 1977.

Received May 29, 2008; revised version October 2, 2008.
